Experimental investigation on a high head Francis turbine model during shutdown operation

IOP Conf. Series: Earth and Environmental Science **240** (2019) 022028 doi:10.1088/1755-1315/240/2/022028

Experimental investigation on a high head Francis turbine model during shutdown operation

R Goyal[1], B K Gandhi[2], and M J Cervantes[3]

[1] Postdoctoral Researcher, Grenoble-INP/CNRS/UJF-Grenoble 1, LEGI, Grenoble, F-38041, France
[2] Professor, Mechanical and Industrial Engineering Department, Indian Institute of Technology, Roorkee, 247337, India
[3] Professor, Department of Engineering Science and Mathematics, Luleå University of Technology, 97187 Luleå, Sweden

E-mail: goel.rahul87@gmail.com

Abstract. Increased penetration of intermittent energy resources disturbs the power grid network. The frequency band of the power grid is normally controlled by automatic opening and closing of the guide vanes of hydraulic turbines. This has increased the number of shutdown cycles as compared to the defined ones for the normal operation of turbines. Turbine shutdown induced a significantly higher level of pressure fluctuations and unsteadiness in the flow field, decreasing its expected life. This paper presents experiments performed on a high head model Francis turbine during shutdown. The pressure and 2D Particle Image Velocimetry (PIV) measurements were performed to investigate the pressure fluctuations and flow instabilities in the turbine. The pressure sensors were mounted in the draft tube cone and vaneless space to measure the instantaneous pressure fluctuations. In the present study, the initial high load operating condition was considered to perform the turbine shutdown. The data were logged at the sampling frequency of 40 Hz and 5 kHz for PIV and pressure measurements, respectively. Time-resolved velocity and pressure data are presented in this paper to show the pressure fluctuations and causes of generation of unsteady flow in the draft tube.

1. Introduction

Normal shutdown of turbine is generally carried out to meet specific conditions such as no electricity requirement, water scarcity, monsoon flood, maintenance purpose, and other safety related issues. The deregulated electricity market and introduction of renewable energies, such as solar and wind have resulted in random and significantly more frequent start-stop cycles of the turbines. Normally, a Francis turbine, operating over the guaranteed efficiency range, is designed to have 1-10 start-stop cycles per year to balance the grid [1]. But the number of start-stop cycles is observed to increase up to 500 per year over the last decades due to increased penetration of intermittent renewable energy sources, and deregulation of energy market [2]. All start-stop costs were observed to be either directly proportional to the number of start-stop or increased with the operating hours of the turbines [3]. Each start-up is observed to cause a wear equivalent to a certain number of operating hours. An individual start-stop cycle is estimated to shorten the refurbishment time period by approximately 15 hours [3-5].

The hydraulic turbines power output is controlled by opening or closing of the guide vanes of a turbine. The angular position of the guide vanes is controlled automatically by a governing servo-motor mechanism as a function of the required power output. The guide vane sequences for normal start-stop conditions are predefined at the time of installation of the turbine and adopted later on during the operation. The increased number of start-stop cycles may lead to an inappropriate opening of the guide vanes, inducing unsteady pressure fluctuations on different components of the turbine.

With the time, the predefined optimum sequence of the guide vanes may behave differently. Consequently, the turbine may experience significant dynamic pressure loading on its components and unsteadiness in the flow downstream the runner which sometimes may be damaging to the turbine [6]. A strong coupling between the pressure amplitudes and operating conditions of the turbine was observed by Kobro [7]. The reduction in vaneless space between the runner blades and guide vanes, and high velocity in the flow passages induce the high amplitude of the rotor-stator interaction (RSI) pressure fluctuations in the turbine. Large pressure fluctuations are developing the fatigue loading on the runner blades. The fatigue loading on the runner blades become more significant during the turbine shutdown. The crack propagation rate on the runner blades due to cyclic fatigue loading is affected by the angular speed of the guide vanes. During a fast movement of the guide vanes, the crack propagation rate is faster as compared to a slower movement [8].

The unsteady flow over a large spatial domain in a Francis turbine raised a scientific interest for the use of Particle Image Velocimetry (PIV). The developed unsteady wakes through the stay vanes, guide vanes, and runner blades were widely investigated at steady-state operations [9-11]. The experiments on hydraulic turbines were mainly performed on reduced scale model turbine due to the limitations associated with the prototype, such as the requirement of standstill condition of the power plant, insertion of the physical probe in the flow domain etc. Furthermore, optical methods are extremely challenging to implement into prototypes due to the material of the structure and machines, restricting any optical access [12]. Researchers [9, 10, 13] employed PIV technique to investigate the flow in hydraulic turbines during off-design operating conditions. Most of the studies were focused on part load (PL) condition to investigate the efficiency drop and pressure fluctuations. The time-resolved velocity components in the radial, axial and tangential directions were analyzed at PL by Tridon et al. [14] and Iliescu et al. [15]. The tangential component of the velocity was significant at PL condition in the draft tube, leading to vortex breakdown. The reason for the efficiency drop was attributed to the development of a complex flow field and vorticity inside the turbine [16-17].

Most of the investigations on hydroelectric turbines focus on the dynamic pressure loading on the runner blades and flow unsteadiness in the vaneless space and draft tube near best efficiency point (BEP). A few studies [6-7, 18] have pointed out that the transient operation like start-stop may greatly affect the life expectancy of the hydroelectric turbines. These investigations have mainly focused on the static and dynamic pressure loading in the vaneless space, runner blades, and draft tube. The vibrations in the turbine during shutdown were mainly explained as the fluctuations resulting from the blade and guide vane passing frequencies of the RSI. However, it may also be associated with the low frequency fluctuations and transient flow condition downstream the runner during shutdown schemes. The resonance between the natural frequency of the runner and developed low frequency fluctuations may also be associated to the vibrations of the turbine. In order to understand in details the impact of a shutdown, synchronized pressure and 2D PIV measurements have been performed on a model Francis turbine. The measurements are performed for different guide vanes openings similar to the prototype operation. In this paper, the effect of RSI has been investigated for one scheme (high load to no load) of turbine shutdown. The investigation of the low frequency fluctuations has been performed for velocity data. The unsteadiness in the flow during transient has been investigated downstream of the runner, i.e., draft tube, during a shutdown scheme from HL operating condition.

2. Material and Method

2.1. Model test rig

A scale (1:5.1) model of a prototype Francis turbine has been selected for the present investigation. The model turbine is installed at the Water Power Laboratory (WPL), Norwegian University of Science and Technology (NTNU), Norway. The prototype turbine (Head =377 m, Power =110 MW, Runner diameter =1.779 m, Discharge = 31 m^3s^{-1}, Runner angular speed =6.25s-1, and Specific

speed=0.27) is in operation at the Tokke power plant, Norway. A schematic of the test rig is presented in figure 1. It is described in detail in the literature [20-23]. The model is composed of 14 stay vanes conjoined inside the spiral casing, 28 guide vanes, a runner with 15 splitters and 15 full length blades, and an elbow-type draft tube. A magnetic flow meter was used to measure the turbine discharge and a differential pressure transducer was used to acquire the pressure difference across the turbine.

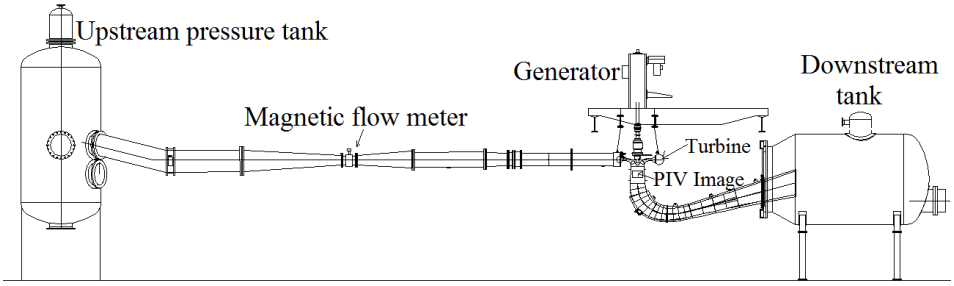

Figure 1. Test rig of the model Francis turbine.

2.2. Pressure and velocity measurements , Instrumentation, and Calibration

The instrumentation, calibration, measurements procedure, and data analysis were carried out according to the guidelines available in International Electrotechnical Commission (IEC) 60041/60193[24-25]. The pressure measurements were recorded using a National Instruments (NI) Compact Reconfigurable Input /Output (cRIO) Model 9074 with a 24 bit analog to digital converter (ADC). The data were sampled at 5 kHz for each channel. The operating and flow parameters such as discharge, turbine inlet and differential pressure, atmospheric pressure, angular speed of the runner, shaft torque to the generator, bearing friction torque, turbine axial force, and guide vanes angular position were acquired through the same acquisition system. In addition to the base instrumentation of the test rig, six pressure sensors (Kistler-701A, 0-25 bar) were mounted in the draft tube cone and two pressure sensors (Kulite-Druck PTX 1830, 0-10bar) were mounted in the vaneless space, one near the beginning of the spiral casing and one near the end as shown in figure 2 and table 1. The estimated uncertainties of the sensors are described in the literature [20-23]. The total estimated uncertainty was ± 0.15% for the hydraulic efficiency under the steady-state operating condition of BEP.

PIV measurements have been performed in the draft tube with a PIV system (TSI). The draft tube cone is made of transparent Plexiglas to allow optical access to the flow domain. The pulsed light sheet with a thickness of ~3 mm, was generated by two Nd:YAG PIV laser with dual cavity performing 100 mJ by the pulse. The wavelength was 532 nm. The lightning field was visualized by a low noise digital charge coupled device (CCD) camera (VC-4MC-M180) of 2048 x 2048 pixel resolution, with a succession of paired images at 300-400 µs. The camera resolution is 2032 x 2048 pixels for a 276.0 x 278.0 mm^2 spatial domain in the present flow domain. Seeding particles (TSI, polyamide 12) were used: particle density of 1.016 g/cc, refractive index 1.52 and mean diameter of 55 µm. To minimize the optical distortion, an index matching box made of glass filled with water, was used for the calibrations and measurements to decrease the light aberration during the PIV measurements. The ex-situ calibration was performed in the draft tube due to practical limitations associated with the in-situ calibrations. A specially designed 2D target plate with dots having a diameter of 2 mm and spaced every 20 mm was placed inside the draft tube for calibration. During the calibration, the camera was at the same position as during the measurements. The random uncertainties in the velocity measurement during steady and transient operations are described in the literature [23]. A sensitivity analysis test with different sampling rate was performed. It was found that at an acquisition frequency of 40 Hz, the light intensity inside the cone was enough for capturing clear images with the CCD camera. 2400 paired images were captured in 60 s at the measurement section.

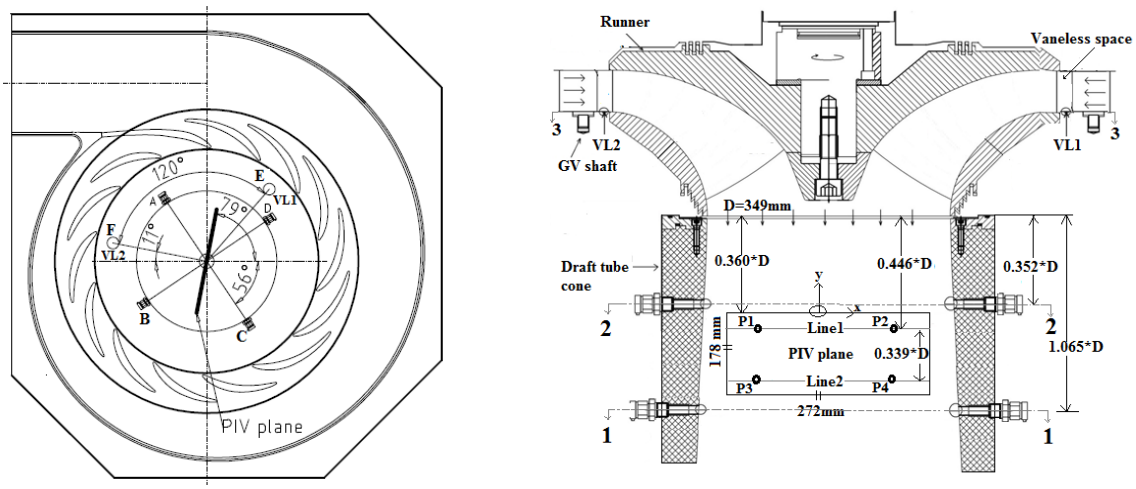

(a) Top view (b) Side view

Figure 2. Pressure sensors placement in the vaneless space (VL1 and VL2) and draft tube (DT1 to DT6) of the model Francis turbine and field of view of the PIV measurements in the draft tube; (a) Top view, (b) Side view. The sensors corresponding to the numbers are shown in table 1; all dimensions are in millimeter; Radial distance of the draft tube and vaneless space sensors are made dimensionless by the runner radius (R=D/2=174.5 mm) and tabulated in table 1.

Table 1. Positions of the pressure sensors.

Sensor	Placement	Radial position (Dimensionless)	Type
DT1	1A	1.12	Kistler
DT2	1B	1.12	Kistler
DT3	1C	1.12	Kistler
DT4	1D	1.12	Kistler
DT5	2B	1.03	Kistler
DT6	2D	1.04	Kistler
VL1	3E	1.23	Kulite
VL2	3F	1.84	Kulite

2.3. Measurement program

Synchronized pressure and velocity measurements were performed on a model Francis turbine during shutdown. The discharge to the Francis turbine is controlled by the guide vanes angular movement. In the investigated model Francis turbine, the guide vanes angular position 0° corresponded to the no discharge condition, i.e., 0% guide vanes opening (GVO), and 14° to the maximum discharge condition, i.e., 100% GVO. Two steady-state operating points were selected for the transient measurements: one at the minimum discharge (α =0.8°), and one at the high discharge (α =12.4°). The 0.8° (6 % GVO) is the minimum angular position of the guide vanes at which the demagnetization of turbine-generator takes place at the synchronous speed of 333 rpm. This operating condition is marked as no load (NL) condition when the runner is spinning freely and synchronization load (SL) condition when the generator is magnetized. The 12.4° (89% GVO) angular positions of the guide vanes

correspond to high load (HL) condition. The specifications of the operating conditions are shown in table 2. The shutdown from HL is presented in this paper.

Table 2. Specifications of the steady state operating points.

Guide vane angle α (°)	Head H (m)	Flow rate Q (m^3/s)	Speed factor n_{ED} (-)	Discharge factor Q_{ED} (-)	Hydraulic efficiency η (%)
0.8	12.14	0.02	0.18	0.01	20.9
12.4	11.88	0.24	0.18	0.18	91.8

Initially, the turbine was operating at steady-state HL operating condition. The guide vanes were closed up to the minimum position to achieve the minimum load condition of the turbine. The turbine shutdown sequence is divided into two phases in the present study. During phase-I, the guide vanes were closed up to the minimum load condition of the turbine and during phase-II, the guide vanes were fully closed (6-0% GVO) in order to achieve the complete shutdown. In the present paper, the obtained pressure signals (VL1, VL2, and DT1-DT6) were presented only for locations VL1 and DT1 in the turbine.

3. Results and Discussion

3.1. Transient Pressure Variation

Figures 3-4 show the transient pressure variations in the vaneless space (VL1) and draft tube (DT1) during phase-I and phase-II of the shutdown. The values of α and pressure (P_{norm}) in the figures 3-4 are normalized according to equation below.

$$X[-] = \frac{X - X_{Min}}{X_{\max} - X_{Min}} \tag{1}$$

Absolute maximum and minimum pressure values in the vaneless space and draft tube at critical (steady-state) instances are tabulated in table 3. A steady state absolute pressure value at VL1 was measured to 172 kPa at 89% opening of the guide vanes. The pressure in the vaneless space was following the movement of the guide vanes closing during the phase-I of the shutdown as shown in figure 3. With the closing of the guide vanes, the transient pressure was steadily decreasing and reached to the operating pressure (148 kPa) about 7 s after the end of the transient operation. The maximum normalized pressure fluctuations in the vaneless space were ±0.15 during the shutdown. The high fluctuations in the vaneless space during shutdown might be associated with the closing of the guide vanes and leading to a small vaneless space between the guide vanes trailing edges and runner leading blades.

Steady state absolute pressure value in the draft tube (DT1) was measured to 102 kPa at 89% opening of the guide vanes. Similar to the vaneless space, the high-pressure fluctuations were observed in the draft tube during the phase-I of the shutdown. The high pressure fluctuations during the guide vanes movement from the high discharge conditions might be associated with the high swirling flow in the draft tube which requires some time to settle down as shown in figure 3.

Table 3. Maximum and minimum values of estimated pressure values during shutdown.

Pressure sensor	Phase-I		Phase-II	
	Max	Min	Max	Min
VL1 [kPa]	172	148	148	101
DT1 [kPa]	102	101	102	101

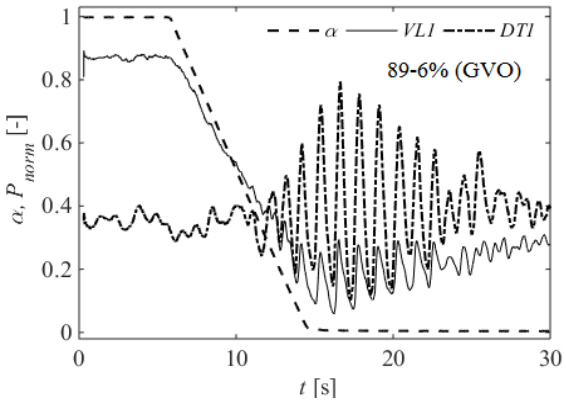

Figure 3. Variation in normalized transient pressure at sensor locations VL1, DT1, and guide vanes closing during phase-I of shutdown.

Figure 4 shows the pressure variation at the same locations during phase-II of the shutdown. The guide vanes were fully closed during the phase-II of the shutdown. Dimensionless pressure amplitudes were steadily decreasing at VL1 with significant instantaneous fluctuations. The absolute maximum and minimum pressure values at location VL1 were 148 and 101 kPa, respectively. The maximum normalized fluctuations (± 0.02) in the vaneless space were corresponding to the transient operating condition of the shutdown. In the draft tube, the pressure variation was complex as compared to that of the vaneless space. The maximum normalized pressure fluctuations at location DT1 were corresponding to the 6% GVO. During the shutdown, the pressure fluctuations were observed to increase as shown in figure 4. The fluctuations were almost 1.5 times of that of the steady-state condition before the transient.

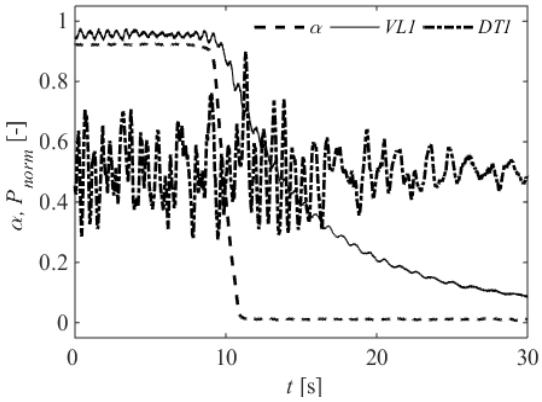

Figure 4. Variation in normalized transient pressure at sensor locations VL1, DT1, and guide vanes closing during phase-II (6-0% GVO) of turbine shutdown.

3.2. Spectral analysis

The maximum pressure fluctuations in the turbine are normally associated with the blade passing frequency in the vaneless space as discussed earlier. Therefore, the spectral analysis of the acquired pressure signal at location VL1 was performed during turbine shutdown. Figure 5 shows the variation of the blade passing frequency at VL1 during phase-I of the shutdown. Initially, the runner was rotating at synchronous speed (333 rpm) with the corresponding steady-state condition. Further, the guide vanes were slowly closed to obtain the minimum load condition of the turbine by maintaining a constant angular speed of the runner. The captured normalized blade passing frequency at VL1 was 30, which was constant during the steady-state operations of the shutdown. Significant fluctuations in blade passing frequency were observed during closing of the guide vane. The fluctuations in this frequency might be attributed to the oscillations in runner angular speed during the transient. A strong power spectral density (PSD) strength of the blade passing frequency corresponds to the high discharge condition may be attributed to a small space between the guide vanes and the runner blades.

The captured blade passing frequency at VL1 was almost constant till the generator demagnetized from the minimum load condition of the turbine as shown in figure 6. The water flowing to the runner and mechanical inertia may have caused the runner to spin continuously even after demagnetizing of the generator, therefore, the blade passing frequency in the vaneless space was observed even after demagnetization of the generator. The blade passing frequency in the vaneless space was observed to decrease with the decrease of the runner speed. The frequency decrease of the blade passing frequency in the vaneless space during turbine shutdown showed an exponential trend with decrease in runner speed. This may be associated to mechanical inertia induced in the runner which rotates the runner even after the complete closing of the guide vanes.

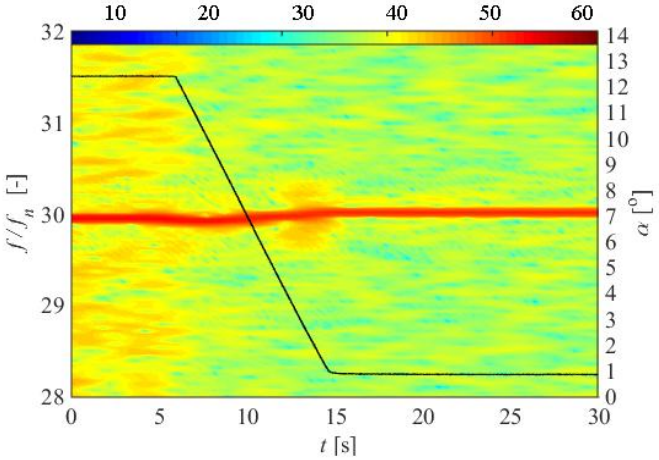

Figure 5. Variation of the blade passing frequency in the vaneless space (VL1) during phase-I of shutdown; black solid line is the guide vanes angle (α) with the y-scale at the right.

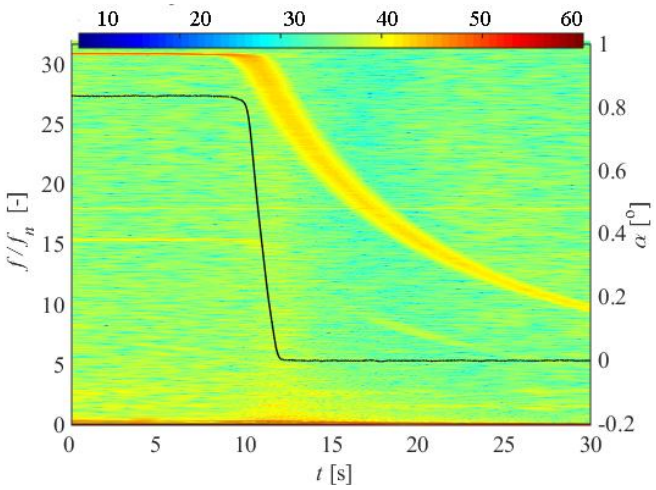

Figure 6. Variation of the blade passing frequency in the vaneless space (VL1) during phase-II of shutdown; black solid line is the guide vanes angle (α) with the y-scale at the right.

The low-frequency fluctuations in the draft tube during turbine transient from 89 to 6% GVO are investigated in the velocity data as shown in figure 7. No significant PSD strength of Rheingans frequency (0.2-0.4.f_n) was observed in the draft tube in between the transient operation from 89 to 6% GVO. However, a significant PSD strength with marginally lower the range of Rheingans frequency is observed at the end of the transient operation as shown in figure 7. This normalized frequency of 0.17.f_n with high PSD strength is appeared in the signal for an almost 9s after the transient stop. However, the effect of this frequency with lower PSD strength continues up to 15s after the transient stop. This low frequency with significant PSD strength (amplitudes) during the turbine shutdown may have some resonance with the system frequency and leading to the development of structural vibration and fatigue loading on the turbine components.

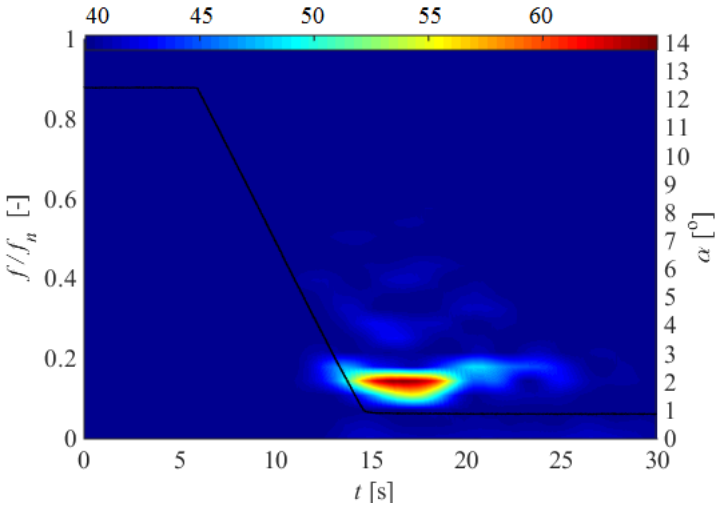

Figure 7. Variation of low frequency in the draft tube for absolute velocity at DT1 during phase-II of shutdown, black solid line is the guide vanes angle (α) with the y-scale at the right.

3.3. Flow Investigation

The instantaneous flow field characteristics of the axial velocity in the draft tube during shutdown (phase-I) is presented to investigate unsteady flow downstream to the runner as shown in figure 8. Initially, the turbine is operating at 89% GVO which corresponds to a HL condition and flow in the draft tube is characterized by a vortex core rotating in a direction opposite to that of the runner. This vortex core rotates around the center axis draft tube. The vortex core has a quasi-dead flow region at the center of the draft tube. As the flow decrease (89-70% GVO), a high axial flow from the runner hub replaces the center dead core and mitigates the vortex core in the draft tube as shown in figure 8. As the flow further decrease (70-48% GVO), a stagnation point appears in the draft tube and separates the flow along draft tube centerline with the flow deceleration as shown in figure 8. The separation of a flow is a condition for the vortex breakdown and in case of a reaction turbine the flow separation in draft tube is leading to the formation of a rotating vortex rope (RVR). In the present study, the draft tube RVR was not observed as fully developed since the turbine discharge starts to decrease continuously up to the no load (6% GVO) condition. However, a frequency of 0.17.f_n with marginally lower than the range of Rheingans frequency was observed in the data at the end of transient operation (see figure 7). Most of the flow during the minimum discharge condition slides through the wall of the draft tube and thus, a positive flow is difficult to capture in the center of the draft tube. Some negative flow regions start to appear in the draft tube as the turbine operation moved towards no load condition. This may be associated with the swirling flow leaving the runner at such minimum opening of the guide vanes. The negative flow regimes may also be associated to the striking of runner flow to the partially filled flow condition of the draft tube at low discharge.

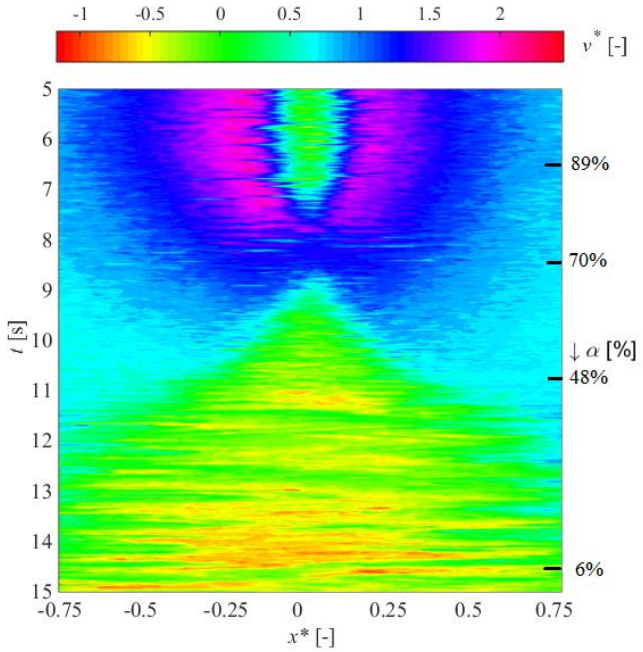

Figure 8. Instantaneous normalized axial velocity (v*) at line1 on the measurement plane during phase-I of shutdown; phase-I refer to guide vanes closing from 89-6%.

Conclusions

The RSI frequency was observed to vary exponentially with the runner speed during the shutdown from no load (6% GVO) to closed (0% GVO) operating condition. The phase-I (89-6% GVO) of the turbine shutdown was observed with high transient pressure fluctuations in the vaneless space and

draft tube. Significant PSD strength was observed at the end of the transient operation for few seconds and normalized frequency ($0.17.f_n$) of this strength was marginally lower the range of Rheingans frequency, but it may be assumed as a vortex rope at minimum opening of guide vanes. Initially, the zero/negative flow regions appear in the draft tube center due to a high load (89% GVO) counter-rotating vortex core. The flow became almost stable for few seconds as the turbine discharge passes the intermittent BEP (70% GVO) condition during the complete shutdown process from 89-6% GVO. A stagnation and flow separation region started to appear in the draft tube as turbine discharge further moves towards the PL (48% GVO) operation condition. Finally some negative flow regimes started to appear in the draft tube as the turbine operation moves towards the no load condition. This may be associated with the swirling flow leaving the runner at such minimum opening of the guide vanes. Some intermittent flow instabilities such as low/dead velocity region and flow separation were captured in the draft tube during turbine shutdown.

Acknowledgement

The measurements have been carried out in collaboration between IIT Roorkee, LTU Sweden, and NTNU Norway. The authors' gratitude goes to the staff of water power laboratory, NTNU, Norway. Special thanks to Prof. Ole Gunner Dahlhaug and Carl Bergan for providing the good measurement facilities. The authors are grateful to the Swedish Water Power Center (SVC) for the financial support. The authors would like to thank the Norwegian Hydropower Centre (NVKS) for the financial support.

References

[1] Huth H J 2005 Fatigue design of hydraulic turbine runners *Ph.D. thesis, Department of Engineering Design and Materials, Norwegian University of Science and Technology, Trondheim*. ISBN: 82-471-6899-5.

[2] Deschênes C, Fraser R, Fau JP 2002 New trends in turbine modelling and new ways of partnership. In: International group of hydraulic efficiency measurement (*IGHEM), Toronto, Canada*, pp 1-12.

[3] Bakken TH, Bjorkvoll T 2002 Hydropower unit start-up costs *IEEE Power Engineering Society Summer Meeting* 3:1522-1527. doi:10.1109/PESS.2002.1043646

[4] Nilsson O, Sjelvgren D 1997 Hydro unit start-up costs and their impacts on short term scheduling strategis of swedish power producers *IEEE Transaction on Power systems* 12(1): 38-44. doi:10.1109/59.574921

[5] Nilsson O, Sjelvgren D 1997 Variable splitting applied to modelling of start-up costs in short term generation scheduling *IEEE Transaction on Power systems* 12(2): 770-775. doi:10.1109/59.589678

[6] Nicolle J, Morissette JF, Giroux AM 2012 Transient CFD simulation of a Francis turbine startup *IOP Conf. Series: Earth and Environmental Science* 15: 062014. doi:10.1088/1755-1315/15/6/062014

[7] Kobro E 2010 Measurement of pressure pulsations in Francis turbines. Ph.D. thesis, *Department of Energy and Process Engineering, Norwegian University of Science and Technology, Trondheim*.

[8] Gagnon M, Tahan SA, Bocher P, Thibault D 2010 Impact of startup scheme on Francis runner life expectancy and reliability. In: *IOP Conf. Series: Earth and Environmental Science* 12:012107. doi:10.1088/1755-1315/12/1/012107

[9] Iliescu MS, Ciocan GD, Avellan F 2008 Analysis of the Cavitating Draft Tube Vortex in a Francis Turbine Using Particle Image Velocimetry Measurements in Two-Phase Flow *Journal of Fluids Engineering*. 130 (2) 021105: 1-10,doi:10.1115/1.2813052

[10] Tridon S, Barre S, Ciocan GD, Tomas L 2010 Experimental Analysis of the Swirling Flow in a Francis Turbine Draft Tube: Focus on Radial Velocity Component Determination *European Journal of Mechanics B/Fluids*. 29 (4): – 321-335, doi: 10.1016/j.euromechflu.2010.02.004

[11] Su WT, Li XB, Li FC, Wei XZ, Han WF, Liu SH 2014 Experimental Investigation on the Characteristics of Hydrodynamic Stabilities in Francis Hydro turbine Models. *Advances in Mechanical Engineering*. 486821: 1-13. http://dx.doi.org/10.1155/2014/486821.

[12] Ciocan GD, Iliescu MS 2012 PIV Measurements Applied to Hydraulic Machinery: *Cavitating and Cavitation-Free Flows-The Particle Image Velocimetry - Characteristics, Limits, and Possible Applications*, May 23, 2012, ISBN 978-953-51-0625-8, doi: 10.5772/35164

[13] Houde S, Iliescu MS, Fraser R., Lemay S, Ciocan GD, Deschênes C 2011 Experimental and Numerical Analysis of the Cavitating Part Load Vortex Dynamics of Low-Head Hydraulic Turbines. *Proceedings Of Asme-Jsme-Ksme Joint Fluids Engineering Conference July 24-29, 2011, Hamamatsu, Shizuoka, Japan*.

[14] Tridon S, Ciocan GD, Barre S, Tomas L 2008 3D Time-Resolved PIV Measurement in a Francis Turbine Draft Tube. *IAHR 24th Symposium on Hydraulic Machinery and Systems, October 27-31, 2008; Foz Do Iguassu, Brazil.*

[15] Iliescu MS, Ciocan GD, Avellan F 2002 3D PIV and LDV Measurements at the Outlet of a Francis Turbine Draft Tube. *ASME 2002 Joint U.S.-European Fluids Engineering Division Conference, July 14–18, 2002, Montreal, Quebec, Canada*; 1: 311316, doi:10.1115/FEDSM2002-31332.

[16] Dorfler P, Sick M, Coutu A 2013 Low-frequency phenomena in swirling flow. In: Springer handbook of flow-induced pulsation and vibration in hydroelectric machinery, *Springer-Verlag, London*, pp 33-67

[17] Favrel A, Muller A, Landry C, Yamamoto K, Avellan F 2015 Study of the vortex-induced pressure excitation source in a Francis turbine draft tube by particle image velocimetry. *Experiments in Fluids* 56:215, doi: 10.1007/s00348-015-2085-5.

[18] Trivedi C (2014) Experimental and numerical investigations on steady state and transient characteristics of a high head Francis turbine. Ph.D. thesis, *Mechanical and Industrial Engineering Department, Indian Institute of Technology, Roorkee, India*.

[20] Goyal R, Bergan C, Cervantes MJ, Gandhi BK, Dahlhaug OG 2016 Experimental investigation on a high head model Francis turbine during load rejection. *IOP Conf. Series: Earth and Environmental Science* 49:082004. doi:10.1088/1755-1315/49/8/082004

[21] Goyal R, Gandhi BK, Cervantes MJ 2017 Experimental study of Mitigation of a spiral vortex breakdown at high Reynolds number under an adverse pressure gradient. *Physics of Fluids (AIP)*, Vol. 29, pp. 104104-1-19.

[22] Goyal R, Cervantes MJ, Gandhi BK 2017 Vortex rope formation in a high head model Francis turbine. *ASME Journal of Fluids Engineering* 139 (4): 041102-1-14. doi: 10.1115/1.4035224

[23] Goyal R, Gandhi BK, Cervantes MJ 2017 Particle image velocimetry measurements in Francis turbine-A review and application to transient operations. *Renewable & Sustainable Energy Reviews* 81 (2), pp. 2976-2991.

[24] IEC 60041 1991-11 Field acceptance tests to determine the hydraulic performance of hydraulic Turbines, storage pumps and pump-turbines *International Electrotechnical Commission* (*Geneva, Switzerland*)

[25] IEC 60041 1991-11 Hydraulic turbines, storage pumps and pump turbines- model acceptance test *International Electrotechnical Commission* (*Geneva, Switzerland*)